PAN
POLSKA AKADEMIA NAUK

M&MS

ANALYSIS AND DESIGN OF A NOVEL TARGET CODING METHOD FOR A PORTABLE COORDINATE MEASUREMENT SYSTEM

**Lingjian Zhu[1), Min Zhao[1), Shangwei Yang[2), Yaokun Huang[2), Huan Jiang[1),
Xing Qin[1)**

*1) School of Mechanical and Precision Instrument Engineering, Xi'an University of Technology, Xi'an 710048, China
(✉ 1733237594@qq.com)*
2) Guangdong Institute of Metrology, Guangzhou 510405, China

Abstract

The target coordinate measurement system features an extensive range of key applications. In many high-precision measurement systems wide scope, high precision and multiple cameras are used. However, the objective of this paper is to enhance the measurement accuracy and range of a monocular target owing to its portability and convenience. A systematic simulation of linear, planar and stereo target structures was carried out to investigate target structures. Based on our simulation results, the 3D target is more accurate and robust to tilt due to rich information available from 3D locations of the markers. To overcome the limitation in the measurement range for the monocular target, ideas of coded stereo target are presented in this paper. The measured coordinates can be calculated from only part of the markers, effectively enlarging the measurement range at short object distances. A stereo coded target system is designed based on this method and is compared to an ordinary monocular target. Stability experiments were conducted under different object distances and poses, which have shown that the Z direction accuracy of the stereo target is at least 23.8% or 10% higher than that of the 1D or 2D target, respectively. Additionally, the ranging experiment revealed that the measurement accuracy of the coded stereo target is 23.5% or 59.2% higher than that of the non-coded 1D or 2D target when measuring the Z direction and the distance of the far field.

Keywords: Portable coordinate measurement system, target structure, coded stereo target, high precision target measurement.

1. Introduction

The portable coordinate measurement system has gained significant attention in recent times. Handheld targets serve as imaging objects in these systems, and images are captured while the target contacts the measured point. By analysing the imaging of known markers on the target, the spatial position of the measured point can be determined [1]. Moving the target probe on the surface of the object enables the acquisition of 3D coordinates of the object surface. This

vision-based detection has advantages such as lightweight, portability, and ease of online operation, making it an increasingly popular option in the precision manufacturing industries [2, 3]. Two commonly used camera types are monocular and binocular ones. The monocular system has a simpler structure and avoids the laborious position calibration and complex image matching process associated with binocular systems. Consequently, it is more convenient for industrial field measurement scenarios [4, 5]. The measurement range is proportional to the size of the target and the measurement accuracy is closely related to the calculation precision of the marker centres on the target, which depends on the number of visual sensor pixels covering the target. As a result, it is challenging to obtain high measurement accuracy for a large range in practice. Hence, this work aims to improve the accuracy of the portable coordinate measuring system while considering high accuracy and wide measurement range to promote its wide application.

Numerous studies have been conducted on target coordinate measurement systems. Some researchers have developed high-precision products with a large measurement range using complex dual-camera or multi-camera structures. The Solo and Duo systems, designed by Metronor, use a 3D target structure and a large view camera. The former has a precision of ±0.188 mm within 10 m, while the latter achieves ±0.060 mm within 10 m and ±0.020 mm within 2.5 m, respectively [6]. Similarly, KEYENCE Japan has also developed similar products. The WM-3500 system utilizes a complex three-camera structure comprising a mobile camera, a probe search camera, and a reference camera, achieving ±10 μm within 6 m for horizontal measurement. Meanwhile, the XM-5000 also employs a dual-camera structure to achieve an accuracy of ±3 μm within 1.2 m for horizontal measurement. The Handyprobe (NEXT) portable light pen *coordinate measuring machine* (CMM) system, developed by Creaform, boasts an impressive accuracy of 0.025 mm within a 10 m range. This is achieved through the use of complicated C-Track dual-camera sensors. However, there is a growing interest in developing high-performance CMM systems that do not require large, high-precision, or costly cameras. Research has shown that the accuracy of the measurement is closely related to the structure of the target, but there is a lack of guidance on how to design target structures with these considerations in mind. To address this gap in knowledge, this paper systematically studies the effectiveness of various target structures, including 1D, 2D, and 3D targets. While the targets used by Metronor, KEYENCE, and Creaform are 3D targets, there is little research on the impact of target structure on measurement accuracy. Huang [7] and colleagues designed a 1D linear target based on the three-point perspective principle. The maximum cumulative measurement error along the Z axis was found to be 0.26 mm within 450 mm. More recently, Wu [8] and colleagues designed a 3-point planar target that was combined with a light field camera. This achieved a maximum error of 0.55, 0.44, and 0.32 mm in the X, Y, and Z directions. Wang [9] designed a 13-point 3D target with triangular markers fixed on the measuring arm of the CMM. This allowed for the establishment of a separate coordinate system for each control point, resulting in a precision of 30 μm. The research of various target structures indicates that the target structure has an important impact on measurement accuracy. The research presented in this paper indicates that 3D structures [10, 11] have higher precision and are more robust to tilts during measurement than 1D or 2D structures. Furthermore, the paper presents ideas for encoding the markers of targets, such that it is possible to measure only part of the markers and still obtain the final result. This effectively extends the measurement range of the CMM system.

The analysis and design of novel target structures require comprehensive simulation of all available options. Our research and simulations suggest that the 3D target structure provides higher accuracy and robustness to tilting due to the additional information that can be gathered from the markers located in 3D space. To address the limitation of the measurement range for monocular targets, we propose the use of coded stereo targets. By encoding the locations of markers, we can select the imaging field of the target and measure objects at short distances without requiring each

marker to be within the range of the imaging field. Based on this idea, we designed a stereo coded target and tested its performance. Our stability and ranging experiments demonstrate that the stereo coded target provides significantly better system performance and measurement accuracy than the 1D or 2D ordinary targets.

The contributions of this paper are as follows:

1. To investigate the impact of structural differences on measurement accuracies, a comprehensive simulation scheme was performed, which included all three types of structures: 1D, 2D, and 3D. The results indicated that the 3D target possessed higher accuracy and was less vulnerable to tilt due to its richer information, providing a foundation for the improvement of the system.
2. Considering the limited measurement range of the 3D target, a coding method was proposed to select the imaging range according to different perspectives, thereby effectively expanding the measurement range of the system. Based on this, a stereo coded target was designed and a stereo coded target coordinate measurement system was constructed.
3. Based on measuring models of targets, the analysis method of target structure is given. So different targets can be designed according to different measurement requirement.

The paper is structured as follows: Section 2 analyses the simulation and analysis methods and results for three different types of target coordinates. Section 3 outlines the design of the stereo coded target, while Section 4 provides a detailed description of the stability experiment and ranging experiment. Finally, Section 5 presents the conclusions.

2. Targets structures and simulations analysis

In the field of target measurement, the structure of a given target is intricately related to its performance. This section analyses the influence of object distance, target angle and other factors on the measurement accuracy according to the simulation of target coordinates of different structures, and proposes the design of coded targets to achieve a relatively large range of coordinate measurements.

2.1. Measuring models of targets

The spatial model of handheld target coordinate measurement is shown in Fig. 1.
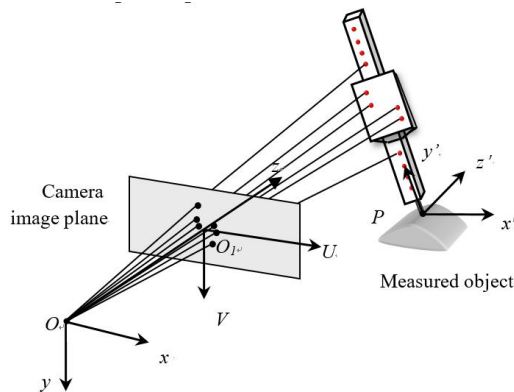

Fig. 1. Spatial model of handheld target coordinate measurement.

Taking the target probe point P as the origin, the target coordinate system $P - x'y'z'$ is established. The coordinates of the marker point on the target are known. The image coordinate system is $O_1 - UV$, with the camera optical center O as the origin, the x-axis and y-axis are parallel to the U-axis and V-axis of the image coordinate system respectively, and the camera coordinate system $O-xyz$ is taken as the measurement coordinate system. During measuring, the target probe P is in contact with the measured object, and the camera collects the image of the markers on the target, and then we obtain the spatial position of the target probe after image processing and spatial coordinate transformation [12, 13].

Suppose the camera focal length f, coordinates of the multiple marker points in the target coordinate system (x_i', y_i', z_i') and their corresponding image point coordinates (U_i, V_i) (corrected by distortion) are known, we can find the unknown parameters such as rotation, translation matrix, and *etc*. by (1) [12].

$$\rho \cdot \begin{bmatrix} U_i \\ V_i \\ 1 \end{bmatrix} = \begin{bmatrix} f & 0 & 0 \\ 0 & f & 0 \\ 0 & 0 & 1 \end{bmatrix} \cdot \begin{bmatrix} R & T \end{bmatrix} \cdot \begin{bmatrix} x_i' \\ y_i' \\ z_i' \\ 1 \end{bmatrix}. \tag{1}$$

In (1), T is the translation matrix between the target coordinate system and the camera coordinate system. These are the 3D coordinates of the origin of the target coordinate system in the camera coordinate system.

If the target probe is the origin of the target coordinate system, the 3D coordinates of the target probe in the camera coordinate system, namely the translation matrix T, can be determined. In (1), by expanding the rotation and translation matrix R and T expansion we can obtain linear (2).

$$\rho \cdot \begin{bmatrix} U_i \\ V_i \\ 1 \end{bmatrix} = \begin{bmatrix} fr_1 & fr_2 & fr_3 & fT_x \\ fr_4 & fr_5 & fr_6 & fT_y \\ r_7 & r_8 & r_9 & T_z \end{bmatrix} \cdot \begin{bmatrix} x_i' \\ y_i' \\ z_i' \\ 1 \end{bmatrix}, \tag{2}$$

where $T = (T_x, T_y, T_z)^T$, $r_1 \sim r_9$ are the components of the rotation matrix R.

The targets have 1D, 2D or 3D structures where the markers are distributed along the straight line, on a plane and in 3D space respectively, and the three structures vary in the measurement principles.

In 3D target all the markers are distributed in 3D space, then (2) is used to substitute variables to obtain the linear equation of unknown quantity (3), then the least squares solution of the unknown quantity a_i can be obtained by the six pairs of corresponding points of the object image.

$$\frac{\rho}{T_z} \begin{bmatrix} U_i \\ V_i \\ 1 \end{bmatrix} = \begin{bmatrix} a_1 & a_2 & a_3 & a_4 \\ a_5 & a_6 & a_7 & a_8 \\ a_9 & a_{10} & a_{11} & 1 \end{bmatrix} \begin{bmatrix} x_i' \\ y_i' \\ z_i' \\ 1 \end{bmatrix}. \tag{3}$$

With the orthogonal constraint, the probe coordinates of each component of the translation matrix, namely the target, are solved as follows [13]:

$$\begin{cases} T_z = 1/\sqrt{a_9^2 + a_{10}^2 + a_{11}^2} \\ T_x = a_4 T_z / f \\ T_y = a_8 T_z / f \end{cases} . \tag{4}$$

The components of rotation matrix R are:

$$\begin{cases} r_1 = (a_1 T_Z)/f \\ r_2 = (a_2 T_Z)/f \\ r_3 = \sqrt{1 - r_1^2 - r_2^2} \\ r_4 = (a_4 T_Z)/f \\ r_5 = (a_5 T_Z)/f \\ r_6 = \sqrt{1 - r_4^2 - r_5^2} \\ r_7 = (a_6 T_Z)/f \\ r_8 = (a_7 T_Z)/f \\ r_9 = \sqrt{1 - r_7^2 - r_8^2} \end{cases} . \tag{5}$$

In the actual measurement process, various errors may violate the strict orthogonality of the resulting R, and the T matrix also has large errors, which requires nonlinear optimization. Thus, (6) can be established from (1).

$$\begin{cases} f_{ai} = f\left(r_1 x_i' + r_2 y_i' + r_3 z_i' + T_x\right) - U_i\left(r_7 x_i' + r_8 y_i' + r_9 z_i' + T_z\right) = 0 \\ f_{bi} = f\left(r_4 x_i' + r_5 y_i' + r_6 z_i' + T_y\right) - V_i\left(r_7 x_i' + r_8 y_i' + r_9 z_i' + T_z\right) = 0 \end{cases}, \ i = 1, 2, \ldots N. \tag{6}$$

The objective function established to minimize the sum of squares of spatial coordinate errors is:

$$I\left(r_1, r_2, \ldots, r_9, T_x, T_y, T_z\right) = \sum_{i=1}^{N} \left(f_{ai}^2 + f_{bi}^2\right). \tag{7}$$

The following penalty functions can be constructed from the orthogonality of matrix R:

$$\begin{cases} f_{p1} = M_1\left(r_1^2 + r_2^2 + r_3^2 - 1\right) \\ f_{p2} = M_1\left(r_4^2 + r_5^2 + r_6^2 - 1\right) \\ f_{p3} = M_1\left(r_7^2 + r_8^2 + r_9^2 - 1\right) \\ f_{p4} = M_4\left(r_1 r_4 + r_2 r_5 + r_3 r_6\right) \\ f_{p5} = M_5\left(r_1 r_7 + r_2 r_8 + r_3 r_9\right) \\ f_{p6} = M_6\left(r_4 r_7 + r_5 r_8 + r_6 r_9\right) \end{cases} . \tag{8}$$

The objective function of constrained optimization in (7) can be converted into the optimization of an unconstrained one:

$$I\left(r_1, r_2, \ldots, r_9, T_x, T_y, T_z\right) = \sum_{i=1}^{N} \left(f_{ai}^2 + f_{bi}^2\right) + \sum_{i=1}^{6} f_{pi}^2. \tag{9}$$

According to (9), the Gaussian–Newton's optimization model is established for the optimal solution.

The origin of the probe coordinate system of 1D, 2D and 3D target can be uniquely determined in the measurement coordinate system. The analysis above shows that the measurement model and optimization method are different according to target structures.

2.2. Simulations analysis of targets structures

MATLAB 2018a is used as the simulation tool. In order to simulate the experiment more accurately, the main parameters of the simulation program are set to be consistent with our experimental system. The image surface size of the CCD camera is 12 mm × 10 mm, the pixel size is 5 μm, the focal length of the objective lens is 50 mm, and noise with a standard deviation of 0.1 pixels is added. The distribution length of the mark points on the target is set as l, the distribution width of the mark points as w, and the distribution height of the mark points as h, as shown in Fig. 2. The simulation results of the targets with different structural shapes are as follows:
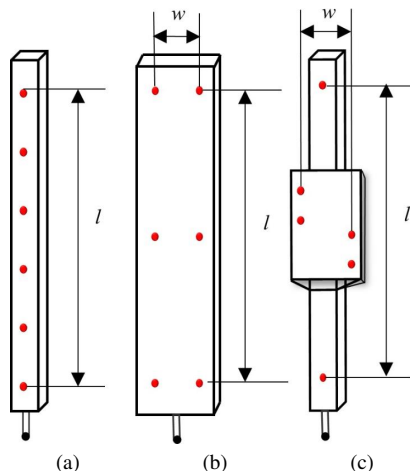

Fig. 2. Common targets with different shapes and structures.

1. Assuming that the 6-point linear target is shown in Fig. 2(a), l is 300 mm, and the relationship between the measured object distance *OD* and the accuracy is shown in Fig. 3, it can be observed that the increase of the object distance results in a precision decrease, which is most evident along the *Z* direction.
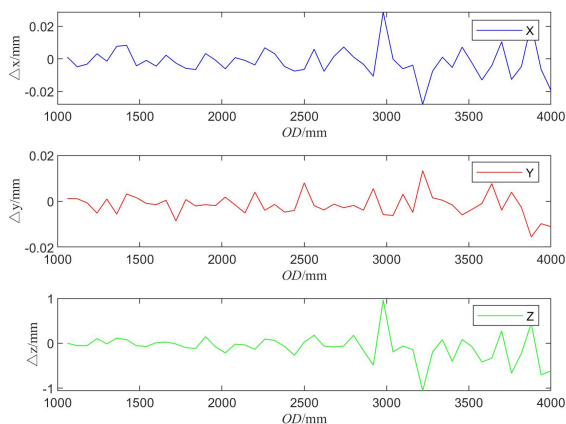

Fig. 3. Object distance vs. accuracy for 1D target.

2. Assuming symmetrical distribution of markers, Fig. 2(b) represents a 6-point 2D target. If *l* is 300 mm, and *w* is 150 mm, the relationship between the object distance *OD* and accuracy is shown in Fig. 4.
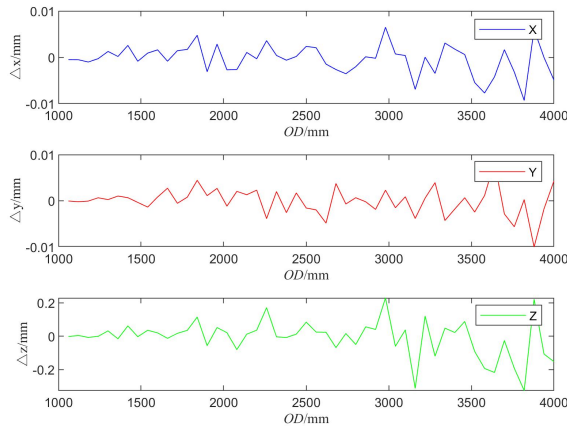

Fig. 4. Object distance vs. accuracy for 2D target.

3. Fig. 2(c) is a 6-point 3D target, and assuming that *l* is 300 mm and *w* is 150 mm, and *h* is 100 mm, the relationship between the object distance *OD* and accuracy is shown in Fig. 5.
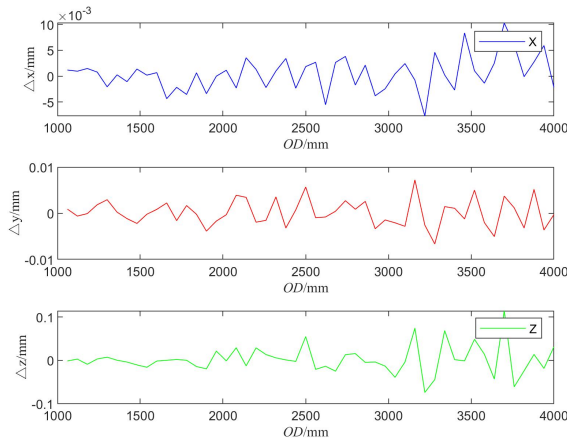

Fig. 5. Object distance vs. accuracy for 3D target.

Comparing Figs. 3, 4, and 5 reveals that the stereo target has a significantly higher measurement accuracy in the *Z* direction than linear and planar targets.

In several scenarios, the target must be tilted to measure the object, which introduces errors. When the object distance *OD* is set to 3 m and certain angles are introduced between the target and the *z*-axis, the relationship between the angle θ and accuracy along the *Z* direction can be obtained, as depicted in Fig. 6. It can be seen that the performance of 1D or 2D targets is severely influenced by increasing the tilt angles, while the precision of 3D targets remains stable. This indicates that 3D targets exhibit more robust performance in situations involving target tilt.
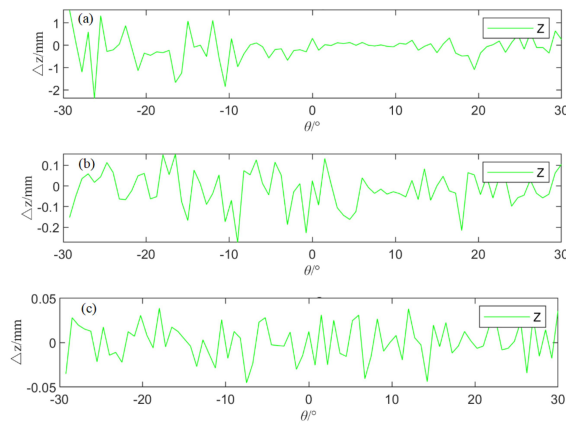
141

Fig. 6. Angle θ vs. accuracy for three targets.

In this study, a 3D target was utilized due to its high precision and resistance to tilting. Simulation results indicate that the accuracy of measurements is minimally impacted by variations in the width w and height h of the stereoscopic target. Thus, widening the target does not significantly improve measurement accuracy. Considering factors such as production, materials, and weight, a width w of 20 mm and height h of 80 mm were selected.

The stereo target used in this study has a width w and height h of 20 mm and 80 mm, respectively, and is placed at an object distance of 3 m. Fig. 7 presents the relationship between the distribution length l of the markers and measurement accuracy. As shown, longer targets result in higher measurement accuracy, particularly in the Z direction, for the same measurement position. Metronor targets utilize a large target combined with a large scope array and a high-resolution CCD to achieve high-precision measurements, and they also employ a long focal length lens. As the measurement distance increases, the target imaging occupies less of the field of view, resulting in a slow decrease in measurement accuracy. However, when using ordinary industrial cameras in the measurement system, employing a large target may not completely capture and measure close-range objects. Furthermore, enabling near-range imaging may result in smaller long-distance imaging and decreased accuracy.
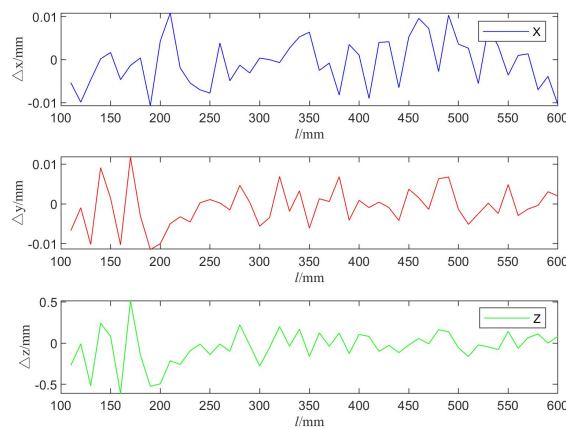

Fig. 7. Stereo target length vs. measurement accuracy.

The longer the target in the camera field of view, the higher the measurement accuracy. However, in practical applications, the length of the target is limited, and the measurement range cannot be expanded by increasing the length of the target indefinitely. Therefore, a unique type of target was considered, wherein the distribution length of markers varies based on the imaging position. The relationship between the *object distance* (*OD*) and accuracy is presented in Fig. 8. The figure demonstrates that while the accuracy slightly decreases with increasing measurement distance, the special target's performance is significantly superior to that of an ordinary linear target. When comparing Fig. 8 with Fig. 5, it is evident that the precision of the special target is considerably better than that of the standard target. Therefore, the design of this special target becomes a key issue.
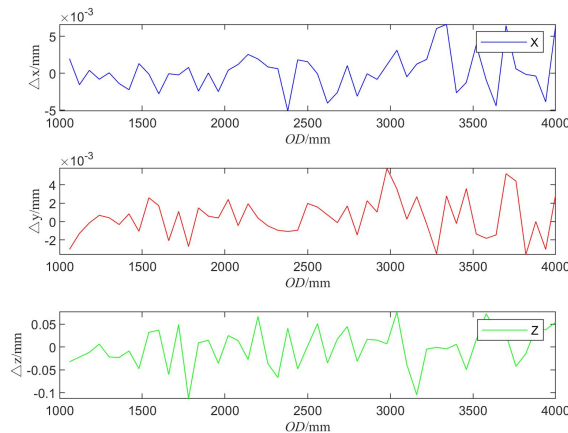

Fig. 8. Object distance vs. accuracy for the special target.

In the proposed method, the coded calibre employs bar codes featuring distinct interval widths, where each possible combination of local bar codes is unique and non-repetitive, enabling determination of their position within the entire code, thus exhibiting the holographic characteristic of the coding method [14]. Motivated by this approach, it becomes feasible to partially code markers within targets, where correct calculations can be performed based on capturing only a portion of the coded target's image at close distances. As the object distance increases, the number of feature points entering the camera's field of view gradually increases, and the distribution of feature points becomes more extensive, thereby maintaining high accuracy. Fig. 9 illustrates the measurement diagram, where CD denotes a coded target and AB represents an unencoded one. When the object distance is l_1, the entire non-coded target AB enters the camera's field of view, resulting in accurate measurement. Meanwhile, the section of the encoded target CD, having the same length as AB, enters the camera's field of view, and the correct measurement can also be obtained following the decoding. During this time, the accuracy of the encoded target is equivalent to that of the unencoded target. However, when the object distance is l_2, the field of view occupied by the unencoded target AB reduces sharply, leading to significant accuracy decline, whereas the encoded target CD occupies a more extensive field of view while still retaining high accuracy, thus enabling high-precision measurement over a relatively wide range.

In summary, 3D targets exhibit superior accuracy and are less susceptible to target tilt. In this study, we propose coded stereo targets built upon the foundation of 3D targets, which enable us to achieve extended measurement range and heightened accuracy.
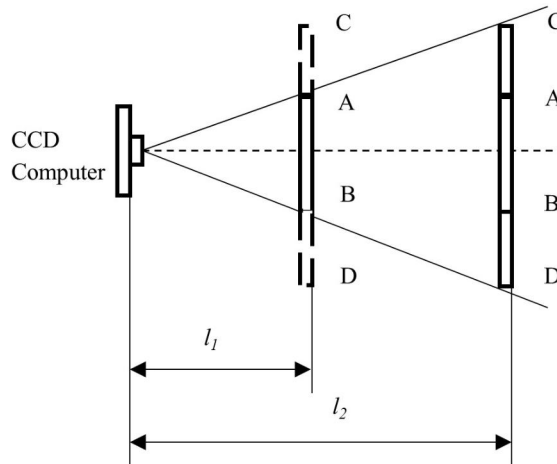
Fig. 9. Measurement schematic.

3. Design of the coded stereo target

The stereoscopic coding target design consists of two parts: the feature point coding and decoding design and the stereoscopic target structure design. The coding feature points with holographic characteristics are designed, and the stereoscopic target structure design is based on simulation to determine the specific parameters of the target, such as length, width, height and feature point distribution, and carry out a mechanical structure design and circuit design to produce the stereoscopic coding target.

3.1. Coding and decoding design

In the field of digital industrial photogrammetry, circular coding and point distribution coding, and *etc.*, are common types of coding markers that are utilized [15, 16]. Circular coding typically comprises a central marker and a concentric coding band. A binary coding scheme is applied, where the coding band is usually divided into 8 coding units. On the other hand, a point-distributed target is mostly composed of markers and coding points. The markers play a crucial role in determining the 2D coordinate system of the target while the coding points are arranged in this planar coordinate system according to specific rules, producing diverse codes. It should be noted that neither circular coding nor point distribution coding is holographic. In the case either of these methods is used as the target coding technique, the entire target needs to be encoded, thus limiting the measurement range expansion. Common coding is often composed of reflective circular signs of different sizes, and the imaging effect is greatly affected by the environment. In this paper, an infrared LED is used as a coding sign, and the size and position of the LED constitute a coding point.

A number of infrared LED light spots with different sizes are used as feature points on the coding target designed in this paper. The large light point with a diameter of 8 mm is the landmark point and participates in the coordinate calculation. The small light point with a diameter of 5 mm is distributed in different positions around the large light point and forms different coding values together with the large light point. When the large light spot is coded 1, as shown in Fig. 10(a), the small light spot located below the right of the large light spot is coded 2, as shown in Fig. 10(b), and the small light spot located below the left of the large light spot is coded 3, as shown in Fig. 10(c).
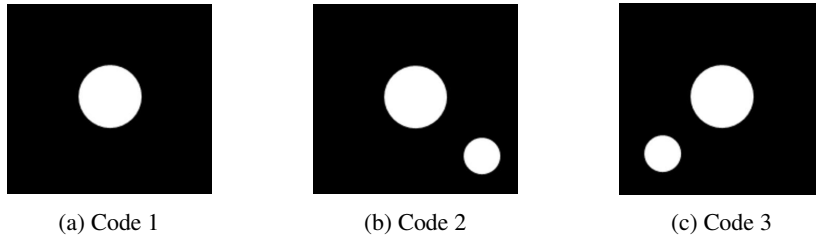
(a) Code 1   (b) Code 2   (c) Code 3

Fig. 10. Schematic diagram of coding.

3.2. Three-dimensional target design

The stereoscopic coding target designed in this paper is shown in Fig. 11. The target consists of two measurement planes, with the lower measurement plane having 8 feature points, distributed in a straight line, and the upper measurement plane has 4 feature points, distributed in a two-dimensional plane. The distribution width of the target feature points is 20 mm, the height of h is 80 mm, and the total length of l is 550 mm. The position of each mark point on the target has been calibrated in the target coordinate system. 6 pairs of corresponding points of the objects above are required to be correctly solved in the measurement principle of stereoscopic target, that is, at least 6 coding points are required to appear in the field of view to solve the coordinates of the measured point when using stereoscopic target measurement. This requires a minimum coding unit of 6 coding points, so the design requires any adjacent 6 coding points to have uniqueness and non-repeatability in the overall coding, so the coding arrangement combination of 12 feature points is designed as: 313312213111. Step holes are used to locate feature points, and the dimensions of step holes are shown in Fig. 12(a). Holes are drilled on the measuring surface so that the LED can be fixed in the hole. As shown in Fig. 12(b), the LED can emit circular light spots through the round holes. In addition, the LED uniform light film is pasted on the measuring surface to obtain a bright, uniform feature point image with high signal-to-noise ratio.

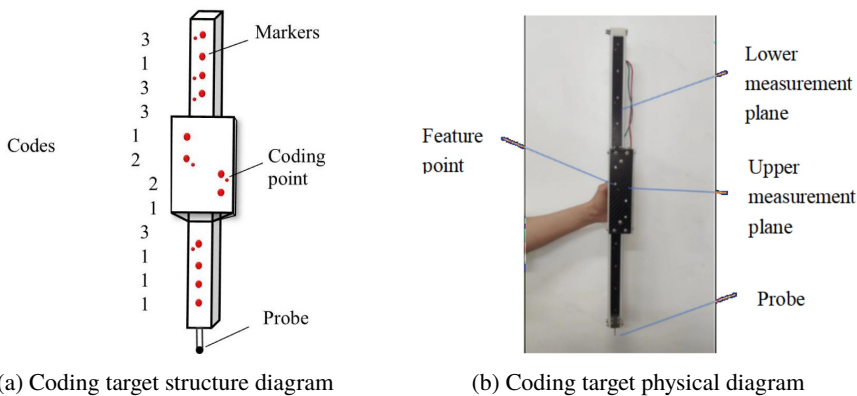(a) Coding target structure diagram   (b) Coding target physical diagram

Fig. 11. Coding target structure and stereoscopic coding target.

Prior to conducting measurements, the position of each marker in the target coordinate system is calibrated. Subsequently, using the acquired target image, the centre of each marker is determined, which then determines the codes based on the relative position of the marker centres. By searching

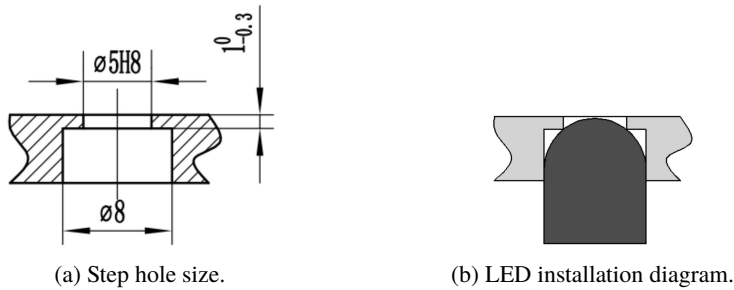(a) Step hole size. (b) LED installation diagram.

Fig. 12. Schematic diagram of step hole and LED installation.

the location of the local codes within the entire code sequence, *i.e.*, the precise location of each marker in the coordinate system, the position of the probe at the object surface can be calculated. To enhance measurement resolution, a small local view field is utilized for imaging. Moreover, the position of the measured point is obtained by determining the position of the target within a relatively large range, thus effectively addressing the conflict between high precision and large range.

4. Experiment

The measurement system utilized in this study comprises a coded stereo target and a JAI industrial camera equipped with a 50 mm prime lens. The camera utilized in this study possesses a resolution of 2560×2048 pixels and a pixel size of 5 μm. Before the commencement of the measurement, all internal parameters (equivalent focal length, camera main point, distortion factor) were calibrated. The coded target utilized in this study possesses a length, width, and height of approximately 600 mm, 20 mm, and 80 mm, respectively, with markers on the target previously calibrated using a coordinate measuring machine. In this study, we conducted a stability experiment and a ranging experiment to further investigate the performance of the measurement system.

4.1. Stability test

To verify the stability of our target, we compared the outcomes obtained from all three structures across different object distances and poses.

4.1.1. Stability test at different object distances

At distances of approximately 2 m, 3 m, and 4 m, a coded stereo target was placed, and 10 images were acquired at each distance. An example image captured at one of these distances is depicted in Fig. 13(a). Additional images were captured for a 2D and a 1D target, as shown in Figs. 13(b) and 13(c), respectively. To obtain the coordinates of the target in the target system, the centres of the markers were identified, and their coordinates were calculated. These coordinates were then used to obtain the coordinates of surface points on the object. From the experimental image, the values for X, Y, and Z coordinates and their deviations (σ_x, σ_y, σ_z) were calculated, and these deviations are presented in Table 1.

Table 1 presents the data for the 1D, 2D, and 3D targets, which indicates a decrease in measurement accuracy as the object distance increases. This decrease is a result of the reduced field of view of the target as the object distance increases, which in turn leads to reduced accuracy.
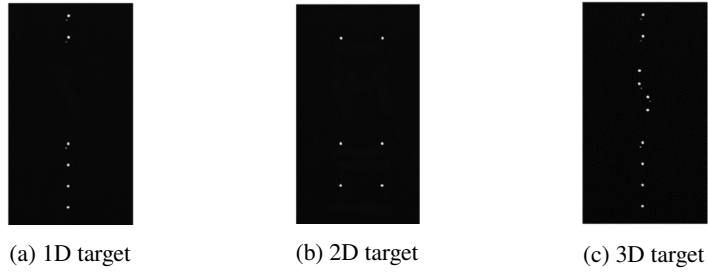
(a) 1D target   (b) 2D target   (c) 3D target

Fig. 13. Images from different targets.

Table 1. Standard deviation of coordinate repeatability under different object distances (unit: mm)

Number	Object distance OD	Target type	X precision σ_x	Y precision σ_y	Z precision σ_z
1	2000	Linear	0.002	0.001	0.033
2	2000	Planar	0.001	0.002	0.024
3	2000	Stereo	0.001	0.001	0.011
4	3000	Linear	0.001	0.003	0.062
5	3000	Planar	0.002	0.001	0.042
6	3000	Stereo	0.002	0.003	0.036
7	4000	Linear	0.007	0.006	0.130
8	4000	Planar	0.009	0.008	0.110
9	4000	Stereo	0.008	0.006	0.099

The standard deviation of the Z direction, as illustrated in Fig. 14, indicates a decline in accuracy as the object distance increases. However, it should be noted that the 3D target exhibits a marked improvement in accuracy in the Z direction of at least 23.8% and 10% over the 1D and 2D targets, respectively. This improvement can be attributed to the rich information provided by the 3D target.
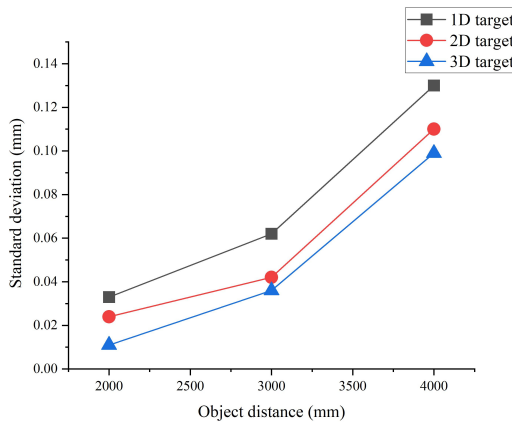

Fig. 14. Standard deviation in the Z direction.

4.1.2. Stability experiments in different poses

The target was placed at an object distance of 2.5 m, and 10 images were captured as the target was tilted by 20°in various directions relative to the camera. The resulting coordinates and deviations are presented in Table 2.

Table 2. Standard deviation of coordinate repeatability in different postures (unit: mm)

Number	Target type	Target attitude	X precision	Y precision	Z precision
1	Linear	Forward tilt 20°	0.001	0.005	0.096
2	Planar	Forward tilt 20°	0.003	0.002	0.053
3	Stereo	Forward tilt 20°	0.002	0.002	0.048
4	Linear	Backward tilt 20°	0.012	0.029	0.362
5	Planar	Backward tilt 20°	0.004	0.008	0.126
6	Stereo	Backward tilt 20°	0.003	0.002	0.032
7	Linear	Left tilt 20°	0.004	0.002	0.089
8	Planar	Left tilt 20°	0.004	0.004	0.053
9	Stereo	Left tilt 20°	0.005	0.005	0.044
10	Linear	Right tilt 20°	0.004	0.006	0.121
11	Planar	Right tilt 20°	0.002	0.005	0.072
12	Stereo	Right tilt 20°	0.004	0.003	0.047

Table 2 evidently indicates that the 3D target outperforms the 1D and 2D targets when tilt is present during measurement. Specifically, the precision in the Z direction is 50% and 9.4% higher than that of the 1D and 2D targets, respectively. Furthermore, the precision decreases as the degree of tilt increases, and it was found that the proposed system works optimally at a tilt angle of 20°.

4.2. Ranging experiment

To assess the ranging performance of the coded stereo target in comparison to non-coded targets, an experiment was conducted. A total of four points were fixed as indicated in Fig. 15. The distance between each point was measured by a high-precision CMM with a precision smaller than 0.01 mm, which is considered the ground truth. All markers on the coded stereo target, both large and small, were imaged for the evaluation. In addition, the non-coded stereo target was utilized, with all markers captured for imaging. The experimental procedure is shown in Fig. 16. The results of the comparison are presented in Table 3, while the measurement error is illustrated in Fig. 17.

Table 3. Ranging results of different targets (unit: mm)

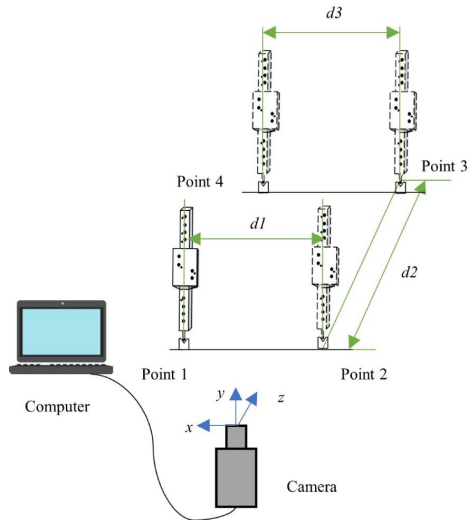| Number	Target type	Deviation from true value	Measuring distance	Error
1	Coded 3D	$d1 = 170.401$	$d1' = 170.362$	0.039
2	Non-coded 3D	$d1 = 170.401$	$d1' = 170.362$	0.039
3	Coded 3D	$d2 = 435.834$	$d2' = 435.926$	0.091
4	Non-coded 3D	$d2 = 435.834$	$d2' = 435.953$	0.119
5	Coded 3D	$d3 = 170.960$	$d3' = 170.911$	0.049
6	Non-coded 3D	$d3 = 170.960$	$d3' = 170.835$	0.125

Fig. 15. Ranging experiment.
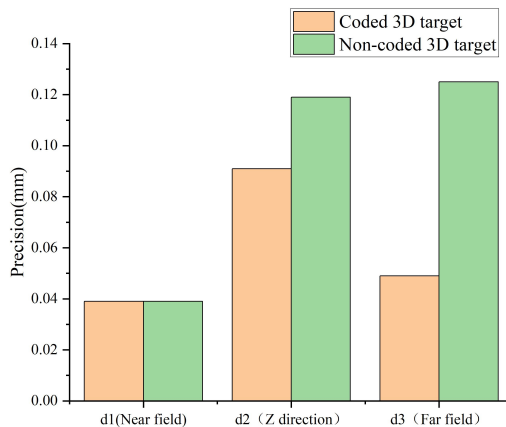

Fig. 16. Experimental process.

Fig. 17. Measurement precision for the ranging experiment.

According to the findings presented in Table 3, it can be concluded that the coded and non-coded stereo targets exhibit similar precision for short object distance *d1*, as the markers occupy the same field of view. However, for object distances *d2* and *d3*, the coded target outperforms the non-coded target, with an improvement of 23.5% and 59.2% in the *Z* direction and far field, respectively. This improvement can be attributed to the fact that non-coded targets require all markers to appear in the field of view. As the object distance increases, the field of view occupied by non-coded targets decreases, leading to a significant decline in accuracy. In contrast, for the coded target, the presence of some markers in the imaging view is sufficient for the calculation, allowing for an increased measurement range and improved precision. The results of the aforementioned experiments clearly demonstrate that the coded stereo target outperforms the non-coded targets in terms of range and precision. Therefore, the design of the coded stereo target can be deemed effective for the purposes of this study.

5. Conclusions

The utilization of the target coordinate measurement system has gained prominence in industrial measurement, due to its lightweight, portability, and convenience in measurement. However, there is a pressing need to improve its measurement accuracy and range. Many existing mature products utilize a costly large-area and high-precision multi-camera systems. To address the need for improved measurement accuracy and range of the monocular target system, this paper presents a classification of complex and diverse target structures, and analyses the measurement principles of three target types: 1D linear target, 2D planar target, and 3D stereo target. Furthermore, a simulation analysis method is established for different target structures. The impact of factors such as the measured object distance and tilt angle on measurement accuracy is examined, and the simulation results reveal that the 3D target has superior information, measurement accuracy, and robustness to tilts. To overcome the challenge that the target imaging method requires all feature points to fall within the field of view of the camera at close range, the paper proposes marker encoding ideas, which enable the acquisition of the local codes of the target through measurement. In consideration of the holographic nature of the target, it has been established that only a subset of the marker images is required to determine the coordinates of the measurement points. This property has enabled an expansion of the measurement range. Accordingly, a coded stereo target has been devised for the final examination. Stability experiments conducted at varying object distances have demonstrated that the *Z* direction accuracy of the stereo target surpasses that of the 1D or 2D target by at least 23.8% and 10%, respectively. Similarly, stability experiments conducted under diverse postures have shown that the *Z* direction accuracy of the stereo target is at least 50% and 9.4% higher than that of the 1D and 2D target, respectively. Ranging experiments have further revealed that the measurement accuracy of the coded target is 23.5% and 59.2% superior to that of the non-coded target when measuring the *Z* direction and the distance of the far field. The aforementioned experiments have provided verification that the system performance and measurement accuracy of the stereo coded target are significantly enhanced in comparison to the non-coded 1D or 2D target. This study has thereby undertaken a beneficial exploration towards the improvement of the measurement accuracy and range of the portable target coordinate measurement system.

References

[1] Shan, D., Zhang, C., Zhang, P., Wang, X., He, D., Xu, Y., Zhou, M., & Yu, G. (2022). Self-Calibration method and pose domain determination of a Light-Pen in a 3D vision coordinate measurement system. *Sensors*, *22*(3), 1029. https://doi.org/10.3390/s22031029

[2] Smith, M. L., Smith, L., & Hansen, M. F. (2021). The quiet revolution in machine vision – a state-of-the-art survey paper, including historical review, perspectives, and future directions. *Computers in Industry*, *130*, 103472. https://doi.org/10.1016/j.compind.2021.103472

[3] Hashmi, A. W., Mali, H. S., Meena, A., Khilji, I. A., Hashmi, M. F., & Saffe, S. N. B. M. (2022). Machine vision for the measurement of machining parameters: A review. *Materials Today: Proceedings*, *56*, 1939–1946. https://doi.org/10.1016/j.matpr.2021.11.271

[4] Kim, M., Kim, J., Jung, M., & Oh, H. (2022). Towards monocular vision-based autonomous flight through deep reinforcement learning. *Expert Systems with Applications*, *198*, 116742. https://doi.org/10.1016/j.eswa.2022.116742

[5] Gorpas, D., Politopoulos, K., & Yova, D. (2007). A binocular machine vision system for three-dimensional surface measurement of small objects. *Computerized Medical Imaging and Graphics*, *31*(8), 625–637. https://doi.org/10.1016/j.compmedimag.2007.07.005

[6] Ämdal, K. (1993). Single camera system for close range industrial photogrammetry. *International Archives of Photogrammetry and Remote Sensing*, *29*, 6-10.

[7] Fengshan, H., & Huifen, Q. (2007). Single camera 3D coordinate vision measuring system using a light pen. *Opto-Electronic Engineering*, *34*(4), 69–72.

[8] Wu, J., Li, Z.C., Zheng, J.W., Xu, J., & Yu, Z.J. (2020). Three-Point Light Pen Space Coordinate Measurement Based on Light Field Epipolar Plane Image Ranging. *Acta Optica Sinica*, *40*(5), 105–112. https://doi.org/10.3788/AOS202040.0512002

[9] Wang, S., Liu, S., & Mao, Q. (2020). A CMM-Based method of control point position calibration for light pen coordinate measuring system. Sensors, 20(19), 5592. https://doi.org/10.3390/s20195592

[10] Saif, Y., Yusof, Y., Latif, K., Kadir, A. Z. A., Ahmed, M. B. L., Adam, A., Hatem, N., & Memon, D. A. (2022). Roundness Holes' Measurement for milled workpiece using machine vision inspection system based on IoT structure: A case study. *Measurement*, *195*, 111072. https://doi.org/10.1016/j.measurement.2022.111072

[11] Brambilla, P.; Conese, C.; Fabris, D.M.; Tarabini, M. Metrological characterization of a laser-camera 3D vision system through perspective-n-point pose computation and Monte Carlo simulations. *In Proceedings of the 2022 Optical 3D Metrology, O3DM 2022, December 15-16, 2022, Wurzburg, Germany, 2022*, pp. 17–21. https://doi.org/10.5194/isprs-archives-XLVIII-2-W2-2022-17-2022

[12] Yu, Q., Xu, G., Zhang, L., & Shi, J. (2021). A consistently fast and accurate algorithm for estimating camera pose from point correspondences. *Measurement*, *172*, 108914. https://doi.org/10.1016/j.measurement.2020.108914

[13] Přibyl, B., Zemčík, P., & Čadík, M. (2017). Absolute pose estimation from line correspondences using direct linear transformation. *Computer Vision and Image Understanding*, *161*, 130–144. https://doi.org/10.1016/j.cviu.2017.05.002

[14] Yang, J. Z., & Liu, Z.Q. (2005). Measuring Principle and Verification of Digital Level. *Beijing: Surveying and Mapping Press*

[15] Hattori, S., Akimoto, K., Fraser, C., & Imoto, H. (2002). Automated procedures with coded targets in industrial vision metrology. *Photogrammetric Engineering and Remote Sensing*, 68, 441–446.

[16] Cronk, S., Fraser, C. S., & Hanley, H. B. (2006). Automated metric calibration of colour digital cameras. *The Photogrammetric Record*, *21*(116), 355–372. https://doi.org/10.1111/j.1477-9730.2006.00380.x

Zhu Lingjian received both his B.Sc. and M.Sc. degrees from Xi'an University of Technology in 2001 and 2004, respectively and received his Ph.D. degree from Xi'an Jiaotong University in 2015. At present he is an Associate Professor at Xi'an University of Technology. His main research interests include measurement, control, intelligent information processing and technology.

Yang Shangwei has worked at the Guangdong Institute of Metrology. His field of scientific research field includes geometric measurement, quantum precision measurement.

Huan Jiang is a master's degree student in Instrument Science and Technology, engaged in measurement, control and information processing research.

Zhao Min is an Associate Professor of the School of Mechanical and Precision Instrumentation, Xi'an University of Science and Technology, Ph.D., Master's supervisor, with research interests in optoelectronic testing and computerized measurement and control technology as well as visual measurement technology. She has participated and presented papers at many international conferences. She has also published more than 20 high-level academic papers.

Huang Yaokunhas worked at the Guangdong Institute of Metrology. His field of scientific research field includes geometric measurement, quantum precision measurement, and laser precision metrology.

Qin Xing is a master's degree student in Instrumentation Science and Technology, working on computer vision measurement technology.